Title
A TWO-DIMENSIONAL DIFFUSION LIMITED SYSTEM FOR CELL GROWTH

Authors
Hlatky, L.
Alpen, E.L.

Publication Date
1984-11-01

Lawrence Berkeley Laboratory
UNIVERSITY OF CALIFORNIA

Submitted to Cell and Tissue Kinetics

A TWO-DIMENSIONAL DIFFUSION LIMITED SYSTEM FOR CELL GROWTH

L. Hlatky and E.L. Alpen

November 1984

Donner Laboratory
Biology & Medicine Division

Prepared for the U.S. Department of Energy under Contract DE-AC03-76SF00098

DISCLAIMER

LBL-18677

A TWO-DIMENSIONAL DIFFUSION LIMITED SYSTEM FOR CELL GROWTH

L. Hlatky & E. L. Alpen

Lawrence Berkeley Laboratory
University of California
Berkeley, California 94720

November 1984

A two-dimensional diffusion limited system for cell growth

L. Hlatky & E.L. Alpen

Biology and Medicine Division, Lawrence Berkeley Laboratory,

CA 94720 U.S.A.

Correspondence: E.L. Alpen, above address.

Abstract. A new cell system, designed to supplement multicellular spheroids as tumour analogues, was analyzed theoretically and experimentally. This "sandwich" system is a single layer of cells, subject to self-created gradients of nutrients and metabolic products. Due to these gradients the sandwich system develops a border of viable cells and an inner region of necrotic cells corresponding to the viable rim and the necrotic center of a spheroid. However, sandwiches differ from spheroids in several ways. All the cells in the sandwich can be microscopically viewed during the entire experiment. In sandwiches there is no three-dimensional cell to cell contact. Also, the gradients are less steep in our sandwich system so the width of the viable region in a sandwich is about ten times as large as the width of the viable rim in a spheroid. Indeed, in sandwiches the experimenter has some control over the steepness of the gradients and can thus vary the width of this viable border. We used DNA labelling studies and flow cytometry along with visual observation to analyze the system. Our experiments show that the observed cell necrosis, similar to that found in spheroids, is due to diffusion limitations. The results are consistent with the idea that oxygen deprivation stops cell cycling and, when extreme and prolonged, leads to necrosis. The possibility that substances other than oxygen are involved is not excluded by the data. The data also suggests that in the final, near-equilibrium state the average overall oxygen

consumption rate for the viable sandwich population may be about one-quarter of that for an exponentially growing population of the same cell line.

INTRODUCTION

The work of Thomlinson and Gray (1955) suggested that the necrosis in tumours might be a direct result of oxygen deprivation, since necrosis appears at a depth in a tumour consistent with the oxygen diffusion distance. Tannock (1968) did an extensive study of the spatial relation of the necrotic regions in mouse mammary tumours to the tumour vascularization; his findings were consistent with such an anoxia hypothesis. Tannock further suggested that limitations in oxygen may also cause viable cells to leave the cycling population thereby reducing the growth fraction to less than unity, as is frequently observed in tumours.

Shortly after Tannock's work the spheroid system was developed as an *in vitro* tumour model (Sutherland *et al.* 1971). In spheroids the geometry is simpler and the external environment is controllable; thus a more detailed check of the oxygen diffusion hypothesis became possible. By the examination of cross sections of fixed spheroids good evidence was found to support the idea that oxygen deprivation plays a major role in the onset of necrosis in spheroids (Carlsson 1979; Franko & Sutherland 1979). In addition this same work also suggests some other factor (nutrient or toxin) may be important.

The present paper describes a new, two-dimensional system, which we have come to call the "sandwich" system. It is, roughly speaking, a living cross section of a spheroid in which all the cells are visible. Sandwiches show the standard spheroid pattern of a cycling outer region, a slowly proliferating middle region and a necrotic center. However, the geometry is such that these regions are greatly magnified. Another difference from spheroids, beside the visibility and amplification of the three regions, is that one has access to the cells in all

regions of the sandwich. One advantage of this access is that in the course of radioactive labelling studies the cells in all parts of the sandwich can be labelled at once, thereby eliminating questions about label diffusion.

In the sandwiches diffusion processes are in effect one dimensional. We can therefore use the diffusion equation in one dimension with an appropriate consumption term to analyse our data, rather than using the three-dimensional equation appropriate to spheroids. This change in dimensionality provides a way to evaluate the current hypothesis that oxygen diffusion limitations cause necrosis. Previous work apart, the results of our sandwich experiments do strongly indicate that necrosis is due to the competition between diffusion of some nutrient or toxin (e.g. oxygen, glucose, lactic acid,...) and the consumption or production of this substance by the cells. Our results are consistent with oxygen being this substance, though they do not exclude the possibility of cooperative effects.

We also used the diffusion equation to check the hypothesis that oxygen deprivation causes the increase in quiescent cells that is seen as the sandwich ages. Our results are consistent with this hypothesis but at present the accuracy of the measurements is not sufficient to confirm it. Since this is a new system, considerable improvements in accuracy can be anticipated.

With further experiments it may be possible to make the sandwich system yield a large amount of information about diffusion, consumption, and the actions of various substances in circumstances similar to those in a three-dimensional vascularized tumour system. Indeed it should be applicable in many other situations where diffusion is the critical factor.

MATERIALS AND METHODS

Cell culture

9L cells from the rat gliosarcoma were used for all experiments. The 9L cell line originated from a N-nitrosomethylurea induced tumour in a CD Fisher rat. The tumour was then developed as an *in vivo-in vitro* tumour model. Our laboratory obtained the initial stock culture from D. Deen (Brain Tumor Research Center, Univ. of California School of Medicine, San Francisco, Ca.).

All cultures were grown in Eagles MEM with Earle's salts (Gibco), supplemented with glutamine, 11% newborn calf serum (Gibco), and 4% fetal calf serum (Irvine Scientific); bicarbonate buffer was added. The oxygen concentration of the air-saturated medium at 37°C was measured to be 0.28±0.04mM using an oxygen electrode (Transidyne General). Cultures were incubated at 37°C in a humidified atmosphere of 5% CO_2 in air.

Stock monolayer cultures were passaged twice a week. Glucose and lactic acid were measured spectrophotometrically using enzymatic assays (Sigma). The pH was measured by standard electrometric methods. These same measurements were always made on the medium of monolayer or sandwich cultures at the time of experiments in order to characterize the medium.

Sandwich system

In the sandwich system, cells are grown in a narrow gap between two glass microscope slides. The cells are grown in a single layer on the bottom slide. A thin layer of medium fills the gap between the slides and separates the cells from the top slide. This sandwiching of cells caused all nutrients and waste products to move into or out of the local environment of the cells by diffusing through the narrow gap between the slides. Cells for both the sandwiches and the control monolayers were seeded at 1×10^5 cells/slide, on 1×3 inch, 1mm thick autoclaved glass slides (Corning). The slides had been placed in 3.5×3.5 inch integrid petri dishes (Falcon), three slides per dish. When pipetting cells

onto the slides an effort was made to distribute the cells uniformly. The slides were then covered with 10 ml of complete medium and incubated at 37°C and 5% CO_2 for 24 hr. After the 24 hr incubation the slides were removed and placed in new dishes. Two slides per dish were held in place using specially designed plexiglass holders and 13 ml of fresh medium was added to cover the slides. This amount was more than enough to insure that the gap between slides was completely filled in all cases.

At this point the density of cells on the slide is still low, $\approx 8 \times 10^3$cells/cm^2. One fourth of the slides were taken to be control monolayer slides and were placed back in the incubator. From the remaining slides, sandwich cultures were formed by the addition of a top slide resting on spacers, sandwiching the cells between slides (Fig. 1). Spacers were of several types: glass, teflon or wire and ranged in vertical spacing dimension from 40 μm to 300 μm. The top slides were treated with prosil-28 (PCR Research Chemicals Inc.), an organosilane nonstick surface coating. This facilitated easy removal of the top slide for thymidine or other labelling studies and similar purposes. Spacers and prosil treated slides were tested and found to be nontoxic to our monolayer cultures. The time of transferring the slides and adding top slides to the sandwiches is referred to as the "setup" time. The age of sandwiches and of their respective control monolayers is measured relative to it.

Note on the figure that the x direction is parallel to the short dimension of the slide, the y direction is parallel to the long dimension, and the z direction is perpendicular to the slide. The gap height Z_g is considerably larger than the height of a single cell layer.

Since medium fills the gap above the cells, one might think that the culture would resemble a monolayer culture rather than a spheroid. However, it is clear that diffusion in the x direction is much slower than it would be if Z_g were

as large as the height of medium above a typical monolayer. Thus, as discussed in more detail below, the competition between diffusion and consumption in a sandwich is quite similar to the same competition in a spheroid. As long as the gap height is small compared to the thickness X_b of the viable border the main effect of having medium in the gap above the cells is merely to decrease the effective number of consuming cells per unit volume, which in turn decreases the steepness of the diffusion gradients.

Measurements of viable cell borders

Integrid Petri dishes containing sandwich cultures were placed directly on the microscope stage and regions of dead cells were identified visually. This visual identification technique for live and dead cells was verified by Trypan blue exclusion. The width of the viable border, X_b, was measured *in situ*, using a Zeiss inverted microscope. These measurements were made at least once a day in order to observe the time dependence of the border. At the time of measurement it was also noted whether the cells were normal looking or had an altered morphology; regions of elongated cells were recorded.

Thymidine labelling index (TLI)

Sandwich cultures grown at several gap sizes, Z_g, were pulse-labelled at various times after setup along with unsandwiched glass slide monolayers. Cells were labelled with the cover slide removed, and then were fixed and developed in place on the slides. Thus labelling was done without disturbing the crucial spatial arrangement of the cells; of course the microenvironment of the cells changes once the glass top is removed. In this way we were able to get a labelling index for each region of the slide, reflecting the influence of pre-existing media gradients. We used short labelling times; therefore it is unlikely that the cell cycle distribution alters during the labelling process.

Sandwich and monolayer slide cultures were labelled using [^{3}H]TdR (6.7 Ci/mmol, New England Nuclear) at a concentration of 0.5μCi/ml. At the time of labelling the media was drawn off the cultures and aliquots from each culture were sampled for the pH and the nutrient state, as discussed under cell culture methods above. The top slide was removed from the sandwich cultures without disturbing the cells attached to the bottom slide. Prewarmed conditioned media containing the label was added to the dishes holding the slides. After preliminary studies, 15 min of 37°C incubation was chosen as the labelling time. Slides were then washed three times in PBS, fixed in 3:1 ethanol:acetic acid, rinsed three times in 70% ethanol, air dried and dipped in Kodak NTB-3 emulsion. After four days of exposure the slides were: developed (Kodak D-19); fixed; and stained with hematoxylin.

The labelling index at different x distances into the sandwich was obtained by division of the viable border into 500μm strips and a thymidine labelling index (TLI) for each of these strips was calculated. This division of the entire viable border into 500μm strips was fine enough in the sense that almost no labelled cells were found in the innermost region and coarse enough that there was a measurable difference between strips. In control monolayers five 500μm strips evenly spaced across the slide were counted. A total of one thousand cells was counted in each strip. A cell was scored as labelled if it had at least ten grains.

Flow cytometry studies

In preparation for flow cytometry, cells were removed from the slides. In the case of the control monolayers, cells were trypsinized off the slides and pipetted repeatedly to achieve a single cell suspension. In the case of the sandwich cultures the removal of the cells involved several steps. First, the top slide was removed. Cells and cell debris from the visually identified necrotic area thereupon floated into the medium and could be flushed off the slide. This left the cells

in the viable border undisturbed, including those with altered morphology. The cells were then trypsinized off and pipetted into a single cell suspension.

Once the cells were in a single cell suspension both control monolayer and sandwich cells were treated following the procedure of Vindelov *et al* (1983) in order to obtain a propidium iodide stained nuclear suspension, as follows. To isolate the nuclei the unfixed cells were digested, using a 10 min trypsin plus sperminetetrahydrochloride (Sigma) in citrate buffer treatment. The sperminetetrahydrochloride stabilizes the nuclei against being disintegrated by the trypsin. After this 10 min treatment, trypsin inhibitor plus Ribonuclease (Sigma) in citrate buffer is added; after another 10 min the propidium iodide (Sigma) in citrate buffer is added. The nuclear suspension is then kept in the dark and on ice for at least 30 min. Immediately before flow cytometric analysis the suspension is filtered through a 50μm mesh.

Flow cytometry was performed with a FACS IV (Becton Dickinson) using the 488nm line of an argon laser. 100,000 flourescent nuclei were collected per histogram. Analysis of the histograms was done using a computer program obtained from Lawrence Livermore Laboratory. The program is the current version of the Dean & Jett (1974) method. In order to evaluate the change in the cell cycle distribution due to sandwich age, sandwiches and their corresponding control monolayers were analyzed at several different times after setup.

Theory

We shall need a sandwich analogue of the mathematical models used for spheroids (Burton 1966; Greenspan 1972; Franko & Sutherland 1979). All models that we have compared to our data involve some form of the diffusion equation

$$\partial f / \partial t = D\nabla^2 f + Qn$$

Here f is the concentration of some key substance such as oxygen, D is the diffusion constant, n is the number of cells per unit volume, and Q is a consumption rate, which could depend on f. We now discuss the simplest model of this kind, which we will call the "basic model". In the basic model the key substance is taken to be oxygen; thus $D=2\times10^{-5}\text{cm}^2/\text{sec}$. There are now four time scales to be considered. The first is the "gap diffusion time" T_g, i.e. the time required for oxygen to diffuse vertically from the top of the gap through the medium down to the cells. $T_g=Z_g^2/D$. For a gap width $Z_g=60\mu\text{m}$ this gives $T_g\approx2$ sec. Next is the "border diffusion time" $T_b=X_b^2/D$ required for oxygen to diffuse horizontally from the outside to the necrotic region. For $X_b=2\times10^3\mu\text{m}$ this gives $T_b\approx\frac{1}{2}$ hr (we give times appropriate for a 60 μm gap width). Third is the "consumption time" T_c during which the cells consume a significant fraction of the oxygen in their own immediate vicinity, $T_c=f/Qn$. For example, if $f=0.28\text{mM}$, $Q=10^{-13}\text{mol/cell-hr}$, $n=10^7/\text{cm}^3$ we get $T_c\approx1/4$ hr. Note that T_c and T_b being of the same order of magnitude is consistent with having a measurable oxygen gradient. Finally there is the time for Qn to double due to cell growth and similar processes; we may take this to be approximately the doubling time of our cells $T_d\approx13\text{hr}$.

We now can list a number of assumptions for the basic model. We assume the term involving time derivatives in the diffusion equation above is negligible compared to the term involving space derivatives. Of course $\partial f/\partial t$ cannot be strictly zero. However in our experiments T_d is large compared to the other times of interest. We can thus regard the system as being in an "adiabatically changing steady state" and taking $\partial f/\partial t=0$ is appropriate.

In the basic model n is taken independent of x and y in the region where n is non-zero. We further take Q to be spatially constant. This assumption is made even for those cells which are viable but, presumably due to low oxygen in their

immediate neighborhood, are not cycling. Also f is independent of y; this merely refers to the directly observed absence of significant edge effects (the very ends of the slides were excluded when making measurements). Furthermore, we assume that cells die whenever the oxygen concentration drops to a critical value f_c; interaction terms due, for example, to cooperation between low oxygen and high lactic acid or other substances are neglected in the basic model.

Finally, one needs an assumption about the z dependence of the oxygen concentration. By analyzing a model in which the oxygen concentration in the medium directly above the cells is different from the oxygen concentration in the volume where cells are present it was found that the difference decays exponentially in time, and that the decay is rapid compared to other times of interest provided diffusion from the top of the gap to the cells below is very rapid. Specifically one needs $T_g \ll T_b$ and $T_g \ll T_c$. In our case these inequalities hold. Therefore we can assume f to be independent of z and we may replace n by N/Z_g , where N is the number of cells per unit area (a constant at any one time by the assumptions above). In this sense varying the gap width Z_g merely corresponds to changing the cell density.

Under these assumptions f is a function $f(x)$ of x alone and one must merely solve the ordinary differential equation $f''=k$ where the constant k is (QN/Z_g) for $0<x<X_b$ and is zero otherwise. The boundary conditions are the following: at $x=X_b$, $f'=0$; at $x=0$, f has the ambient value $f_a=0.28\pm0.04$mM.

The solution for f thus has the form

$$f=f_c+\tfrac{1}{2}k(x-X_b)^2 \qquad (1)$$

in the region $0<x<X_b$ and f is constant in the region where the cells are dead (Fig. 2). Solving Eq. 1 for X_b we get

$$X_b = [2(f_a - f_c) Z_g D / QN]^{1/2} \quad (2)$$

The basic model just described is the one we use to interpret our data. For example we shall vary Z_g to check the proportionality of X_b and $Z_g^{1/2}$. Of course modifying any of the above assumptions leads to different models. For example a model was considered in which n depends on x. This model did not lead to an improved fit with the data, mainly because most of our results refer to comparatively late times while the x dependence of n is most pronounced at early times. Similarly, we considered a model in which cells die only if they have both too little oxygen and too much lactic acid. The oxygen concentration was again described by Eq.1. The concentration of lactic acid was modeled taking into account the fact that lactic acid production is higher when the oxygen concentration is small (anerobic glycolysis). But the model has too many adjustable parameters to be tested critically by the present data.

RESULTS

Doubling time and oxygen consumption in monolayers

To interpret our sandwich results we needed some background data on monolayers, specifically the doubling time and the oxygen consumption. No difference was found for the doubling time, T_d, or the utilization of glucose and lactic acid by the 9L cells when they were grown conventionally in monolayer on plastic petri dishes or in monolayer on glass slides. A T_d of 13.1 hr was observed over the range of exponential growth. The glucose consumption per cell, λ_G, and lactic acid production per cell, λ_{LA} over this range were computed from the cell number measurements and concentration measurements (Figs. 3 and 4). The average values were $\lambda_G = 6.2 \pm 1 \times 10^{-13}$ mol/cell-hr, in agreement with Li's (1982) value for the same cell line, and $\lambda_{LA} = 1.0 \pm 0.2 \times 10^{-12}$ mol/cell-hr. The oxygen consumption rate Q over this range was calculated assuming that all

glucose not appearing as lactic acid goes completely through oxidative phosphorylation, i.e. $Q=6(\lambda_G-\frac{1}{2}\lambda_{LA})$. We found $Q=7.2\pm1\times10^{-13}$moles/cell-hr.

The time and gap dependence of the viable border

Like spheroids, the sandwiches developed three distinct regions: a normal-looking (and cycling) outer region, a morphologically altered (and almost non-proliferating) middle region, and a necrotic center; the first two regions constitute the viable border. We visually studied the time development of this pattern including changes in cell density and the onset and growth of the necrotic region. We also measured the size X_b of the viable border. Sandwiches of different gap sizes all showed qualitative similarities, as follows.

After setup all cells go through one to several doublings (the number depending on gap size). Then a central necrotic region appears abruptly and a sharp demarcation between live and dead cells is observed. At this time one sees a gradient in the cell density (cells/area) over the viable border; cells are more dense at the outer edge of the sandwich and less dense near the necrotic center. Cells adjacent to the necrotic region become elongated, appear pigmented and are presumably stressed; these cells form the middle region. With time the necrotic region expands (i.e. X_b decreases; see Fig. 5) and the density of cells in the viable border increases. About 4 days after set-up the outer cells become confluent; at about this time a final viable border size is reached. This final border size persists for several days without media changes. Although we did not do so for any of the experiments dicussed in this paper, one can keep the sandwiches alive for several weeks by changing the medium twice weekly.

Fig. 5 shows the time dependence of X_b for the case of a 75μm gap. It also shows the time dependence of the distance from the outside of the slide to the start of the stressed (i.e. middle) region. We will call this distance X_s; in other words X_b-X_s is the width of the stressed region. The initial time dependence of

X_s was fit by linear regression on a semi-log plot. This fit is analyzed in the discussion section.

Cells always form a single layer on the bottom slide regardless of the gap size. The viable border width is uniform to an accuracy of about 10% between different slides of the same gap size and within one slide is independent of y to an even higher precision. Visually necrotic cells remain in place and observable during the course of experiments as long as the top slide is not removed.

Although, as stated above, the qualitative features are the same regardless of the gap size, the details can be quite different. The overall effect of increasing the gap size was to spread out effects in space and slow down the onset of necrosis. For example, in 290 μm gap sandwiches the necrotic region did not appear until 56 hr after setup, in contrast to the 60 μm gap preparations where the necrotic center appeared at 10 hr.

Despite differences in the details, the sandwiches all settled down to a near-equilibrium situation when the density was about $N=8.0\pm1.5\times10^4/\,cm^2$. With this N the final border sizes can be estimated theoretically by using Eq. 2. These theoretical values can then be compared to the observed values. The value of f_a is 0.28±0.04 mM, the concentration of O_2 in the air saturated medium at 37°C. In our calculations we take f_c to be negligibly small, although some spheroid work (Carlsson *et al.*, 1979; Franko & Sutherland, 1979) found values corresponding to 10-40 mm Hg. for this quantity. Even using 40 mm Hg. would have only a minor influence on our calculated final border sizes. $D=2\times10^{-5}cm^2/sec$. In choosing a value of Q, we should not naively use the consumption rate for exponentially growing cells since many of the cells are quiescent. Freyer *et al.* (1984) found in spheroids that the average value of Q was 1/4 that for exponentially growing cells. Our system should be similar to spheroids in this respect; that is the average Q should be down. If we adopt the

factor of 1/4 and use the consumption rate for exponential growth given in the section on background monolayer studies our consumption rate Q becomes $Q=1.8\pm0.2\times10^{-13}$mol/cell hr. For the case of $Z_g=60\mu$m this gives $X_b=1300\pm100\mu$m compared to an observed value which is also $1300\pm100\mu$m. The values for the three other gap sizes tested also show this close agreement between prediction and observation. This analysis remains valid even if, as suggested by some of our observations, there is a lag between the time the oxygen concentration reaches f_c and the onset of necrosis (in general, time lags should be easier to observe in sandwiches than in spheroids).

The observed values of the final, near-equilibrium border widths are shown in Fig. 6. The solid curve is a linear regression fit on a logarithmic scale for ease of later comparison with Eq. 2. The slope is 0.53 compared to the slope of 0.50 predicted by Eq. 2.

Labelling index as a function of gap height and of distance x

The two main qualitative results of the labelling experiments were the following: all sandwiches show a decrease in labelled cells as one moves inward on the slide; moreover, the details of this decrease depend on the sandwich gap size. One experiment is shown here to exemplify these findings, which extend to all our labelling experiments. Sandwiches of 60 μm , 180 μm , and 290 μm gap heights were labelled 48 hr after setup. At this time the region over which live cells were found varied greatly in width for sandwiches of different gap sizes. Those of 60 μm and 180 μm gaps showed viable borders approximately 3000μm and 5200μm respectively. The 290 μm gap sandwiches had no necrotic region after 48 hr: live, attached cells were found across the whole slide. At 48 hr none of the borders had reached confluence. The absence of confluence enabled us to look at changes in the TLI due to media gradients without the complication of cells leaving cycle due to confluence.

The cells held their place well on the slide through the entire process of autoradiography. In fact, after labelling, the distance to the region where no cells remained on the slide was 3000 μm and 5000 μm for the 60 μm and 180 μm gap slides respectively, in good agreement with the observation of viable borders. Visually, it was possible to notice a definite gradient of labelled cells over the entire viable region of the sandwiches. Control monolayers showed no such gradient. Fig. 7 shows the TLI *versus* distance into the sandwich. Note that at the outer edge, $x=0$, of all sandwiches the TLI is roughly the same, corresponding to the TLI of 45% that was seen in all regions of the control monolayers. All sandwiches show a steady decrease in the TLI to essentially 0% as one moves from the outside edge of the slide to the inner necrotic region, that is from $x=0$ to $x=X_b$. Although 290 μm gap sandwiches do not develop a necrotic region until 56 hr, the labelling index drops to 0% at 7000 μm. The smallest gap shows the steepest gradient of labelled cells and the largest gap has the least steep gradient.

The curves shown are least square fits to quadratic functions, the slope of which is constrained to be zero at the point where there are no more live cells. This choice of fitting curves is suggested by the model of the preceding section and is discussed in the next section.

For the sandwiches with a 290 μm gap an additional phenomenon was observed. For distances x greater than 3500 μm the average number of grains per labelled cell decreased. This may be due to differences in the intracellular nucleotide pools. That is, before the lid is removed, redistribution of nucleotides from the breakdown of cells in the central region could occur; these nucleotides might be available to the salvage pathway of nearby cells, diluting the effect of the added [^{3}H]TdR.

Cell cycle distributions

Using flow cytometry the cell cycle distributions in sandwiches are found to be between those for exponential and confluent monolayers, and the percentage of cells with a G_0/G_1 DNA content is found to increase as the sandwich ages. Similar results have been reported for spheroids (Allison *et al* 1983).

At setup, slides with an exponentially growing cell population (Fig. 8a) are divided into two groups -- sandwiches and controls. In time the cell cycle distribution for sandwiches then deviates from the exponential pattern (Fig. 8b). Analysis of this FACS data (as discussed in the methods section) gave the results in Table 1. We also include the data for 60μm gap sandwiches at 22.5 hr and that for confluent cultures for purposes of comparison. The decrease in S observed for the sandwiches is not a confluence effect. The 39 hour sandwiches exhibit no visible confluence. Moreover, at 39 hours the control monlayers are still in the exponential growth phase (Fig. 3) and exhibit an exponential cell cycle distribution when analyzed by flow cytometry. The fact that 24% of the cells are in S for 60μm sandwiches at 39 hr appears consistent with the labelling indices shown in Fig. 7 for the 60μm sandwiches at 48 hr.

DISCUSSION

In order to better understand the cell cycle distribution and the development of a necrotic center in poorly vascularized tumours, we developed a two-dimensional, diffusion-governed system for cell growth. Our system complements the spheroid system, a three-dimensional *in vitro* tumour model. Spheroids have been widely used during the last ten years as models for the cellular kinetics (Durand 1976), the radiation response (Sutherland & Durand 1976; Durand 1980), and the growth dynamics (Franko & Sutherland 1979; Yuhas 1978) of tumours. Spheroids are thought to mimic tumours with respect

to both the nutrient diffusion gradients and the three dimensional cellular interactions; of course, spheroids have no vascularization. Phenomena that are observed in tumours and spheroids alike, but not in conventional monolayer cultures, are thought attributable to either diffusion gradients, three-dimensional contact or some combination of these. If these phenomena are also observed in sandwich cultures they should be viewed as a result of gradients, since the sandwich system does not have the three-dimensional cellular interactions present in spheroids.

Our sandwich system is in this respect less like a tumour than is a spheroid, but it has the advantage that it gives optimal information on diffusion effects in growing cell populations. The amplification of the viable border by a factor of ten, compared to viable rims in spheroids of the same cell line, points to the increase in cell kinetic information available from labelling studies on sandwiches. That is, since the gradients of diffusing substances are less steep, there are many more cells within a given concentration range and one can separate out sub-populations more easily.

One also has control over the border width by simply varying the gap height. This allowed us to check the causal relationship between diffusion and necrosis in a way not available in the spheroid system. We varied the sandwich gap height and observed different final border widths (Fig. 6) for the same cell line under the same initial conditions. That necrosis is the result of diffusion limitations seems clear from the 0.53 slope observed. Not only our basic model, in which the key substance is oxygen, but also any other simple diffusion limited model predicts a 0.50 slope for that curve since Eq. (2) implies $\ln X_b = \frac{1}{2}\ln Z_g + A$, where A is independent of Z_g.

If the key substance is oxygen we can obtain a value of Q using Eq. 2 and the values $f_a = 0.28 \pm 0.04$mM, $f_c = 0$, $D = 2\times10^{-5}$cm^2/sec, $N = 8.0 \pm 1.5\times10^4$/cm^2 already

discussed. Using the best fit line in Fig. 6 to average, we get $Q=2f_a DZ_g / NX_b^2 = 1.65\pm0.3\times^{-13}$mol/cell-hr. Since this is indeed about (1/4) the value of Q found for exponential growth, just as in spheroids (Freyer *et al.* 1984) the oxygen assumption is consistent.

Several investigators (Mueller-Kleiser *et al.* 1983; Li 1982) have suggested that glucose, as well as oxygen is a critical factor in the onset of necrosis under certain conditions. A calculation similar to that just given for the case of oxygen determines the glucose consumption λ_G needed to account for the observed border widths if glucose alone were the limiting factor. In contrast to the spheroid case we can use the glucose diffusion constant for medium, without considering cell packing density. We find $\lambda_G \approx 10^{-12}$mol/cell hr, i.e. about twice the value found in exponential monolayer growth for our cell line.

The increase observed in non-cycling cells as the sandwich ages parallels the findings of non-cycling cells in large spheroids (Allison *et al.* 1983; Carlsson 1979; Durand 1976) and in poorly vascularized tumours (Tannock 1968). There is the typical decrease of cells in S as we move away from the nutrient source, reaching 0% near the necrotic region. This is shown directly by [^{3}H]TdR labelling experiments (Fig. 7). In examining Fig. 7 it is worth noting that the dependence of labelling index on the distance x into the slide can be analyzed much more closely in sandwiches than is possible in spheroids because the viable borders in sandwiches are ten times larger than the viable rims in spheroids and one does not need to section the sample to view the labelling index. Due to this extra sensitivity it makes sense to see how well our data fits the hypothesis that cells stop cycling due to low oxygen. There is indeed evidence that cells become quiescent when exposed to low oxygen (hypoxia blocks in G_1; see Koch *et al.* 1973 and also Loffler *et al.* 1978). Olivotto & Paoletti (1981) found that certain quiescent tumour cells could not be brought back into cycle unless

oxygen was available. With this in mind let us return to our basic oxygen model and assume that at a given x the labelling index is simply proportional to $f(x)-f_c$, the amount by which the oxygen concentration exceeds the critical value for necrosis. Then the labelling index should depend quadratically on x; the curvature (i.e. the coefficient C of the term $\frac{1}{2}Cx^2$) should be inversely proportional to the gap width (compare Eq. 1). In Fig. 7 we have given least square quadratic fits under the constraint that the slope go to zero at an appropriate point near the necrotic center. The corresponding values of C, namely 4.7 for $Z_g=60\mu m$, 3.0 for $Z_g=180\mu m$ and 0.79 for $Z_g=290\mu m$ indeed decrease as the gap height increases. The lack of a direct proportionality to $1/Z_g$ may be due to the fact that labelling is not precisely proportional to the oxygen excess or may be an artifact reflecting the marked sensitivity of our fit to the exact choice of constraints. Because the borders are so wide it should be comparatively easy to supplement the data in Fig. 7 and investigate this question more closely.

Visually, the middle region of the sandwiches (between X_s and X_b) contains cells showing an altered morphology. This phenomenon of "visible stress" and that of cell quiescence are presumably closely related, though by no means identical. Thus we should also try checking the hypothesis that cells become visibly stressed due to low oxygen. More specifically, suppose that cells show this altered morphology wherever the oxygen concentration falls below a certain value f_s, possibly after a time lag t_l, and that the consumption by cells in the middle region is negligible compared to consumption by cells in the outside region. Then we can use Eq. 2 to evaluate the behavoir of X_s by replacing f_c and X_b with f_s and X_s respectively. This gives $\ln X_s(t)=-\frac{1}{2}ln(QN)+K$ where K is time-independent and QN is evaluated at $t-t_l$. For $N=N_0e^{\alpha t}$ with $\alpha=ln2/13hr$ and Q constant we have $\ln X_s=-\beta(t-t_l)+constant$ with $\beta=ln2/26hr$. Plotting $\ln X_s$ *versus* time in Fig. 5 we can find the empirical value of the slope β. From

the fitting curve, which uses only the first three points to avoid any confluence effects, we obtain $\beta = ln\,2/\,32$hr. The agreement between calculated and empirical slopes is reasonable and the discrepancy could be due to the fact that Q decreases in time rather than being constant. Thus the presence of visibly stressed cells, like that of quiescent ones, might be explainable by an oxygen deprivation hypothesis.

Another example of the increase in quiescent cells as the sandwich ages is given by the FACS data. This data, which gives results integrated over all the cells, from the outer cells to the ones nearest the necrotic center, appears consistent with the labelling data. The FACS data also shows that the decrease of cells in S is accompanied, as expected from spheroid work (Allison *et al.* 1983; Sutherland *et al.* 1971), by an increased fraction of cells in $G_0/\,G_1$.

In summary, our picture of a sandwich after setup is the following. When the top slide is put in place, gradients of oxygen, nutrients and metabolites form. These gradients mean different local environments for cells in different regions of the sandwich; the consequence is a spatial variation in the cell cycle distribution. As the cells multiply the gradients become larger. Cells in the center die, perhaps from lack of oxygen. Cells adjacent to this central necrotic region appear visibly altered, go out of cycle, and ultimately also die. The size of the necrotic region expands and the density of cells in the viable border increases, until a near-steady state is reached. We see that despite the change in geometry there are many salient features that are similar in sandwiches and spheroids but don't appear in normal monolayer cultures. Such features can be considered as consequences, direct or indirect, of diffusion gradients.

ACKNOWLEDGMENTS

This investigation was supported by the Office of Health and Environmental Research of the U.S. Department of Energy under contract No. DE-AC03-76SF00098, and by Research Grant CA15184 awarded by the National Cancer Institute, DHEW. We are grateful to Steve Neben and Jason Wong for their assistance in carrying out the experiments.

REFERENCES

Allison, D.C., Yuhas, J.M., Ridolpho, P.F., Anderson, S.L. & Johnson, T.S. (1983) Cytophotometric measurement of the cellular DNA content of [^{3}H] thymidine-labelled spheroids. *Cell Tissue Kinet.* **16**, 237.

Burton, A.C. (1966) Rate of growth of solid tumors as a problem of diffusion. *Growth*, **30**, 157.

Carlsson, J., Stalnacke, C.G., Acker, H., Haji-Karim, M., Nilsson S. & Larsson, B. (1979) The influence of oxygen on viability and proliferation in cellular studies. *Int. J. Radiation Oncology Biol. Phys.* **5**, 2011.

Dean, P.N. & Jett, J.J. (1974) Mathematical analysis of DNA distributions derived from flow microfluorometry. *J. Cell Biol.* **60**, 523.

Durand, R.E. (1976) Cell kinetics in an *in vitro* tumor model *Cell Tissue Kinet.* **9**, 403.

Durand, R.E. (1980) Variable radiobiological responses of spheroids. *Radiat. Res.* **81**, 85.

Franko, A.J. & Sutherland, R.M. (1979) Oxygen diffusion distance and development of necrosis in multicell spheroids. *Radiat. Res.* **79**, 439.

Freyer, J.P., Tustanoff, E., Franko, A.J. & Sutherland, R.M. (1984) In situ Oxygen consumption rates of cells in V-79 multicellular spheroids during growth. *J. Cell. Physiol.* **119**, 53.

Greenspan, H.P. (1972) Models for the growth of a solid tumor by diffusion. *Stud. Appl. Math.* **51**, 317.

Koch, C.J., Kruuv, J., Frey, H.E. & Snyder, R.A. (1973) Plateau phase in growth induced by hypoxia. *Int. J. Radiat. Biol.* **1**, 67.

Li, C.K.N. (1982) The glucose distribution in 9L rat brain multicell tumor spheroids and its effect on cell necrosis. *Cancer* **50**, 2066.

Loffler, M., Postius, S. & Schneider, F. (1978) Anaeobiosis and oxygen recovery: changes in cell cycle distribution of Ehrlich ascites tumour cells grown *in vitro*. *Virchows Arch. B Cell Path.* **26**, 359.

Mueller-Kleiser, J.P., Freyer, J.P. & Sutherland, R.M. (1983) Evidence for a major role of glucose in controlling development of necrosis in EMT6/Ro multicell tumour spheroids. *Advances Exp. Med. Biol.; Oxygen Transport to Tissue -- IV* **159**, 487.

Olivotto, M. & Paoletti, F. (1981) The role of respiration in tumor cell transition from the noncycling to the cycling state. *Journal of Cellular Physiology* **107**, 243.

Sutherland, R.M., McCredie, J.A. & Inch, W.R. (1971) Growth of multicell spheroids in tissue culture as a model of nodular carcinomas. *J. Natl. Cancer Inst.* **46**, 113.

Sutherland, R.M. & Durand, R.E. (1976) Radiation response of multicell spheroids -- an *in vitro* tumour model. *Curr. Top. Radiat. Res.* 11, 87.

Tannock, I.F. (1968) The Relation between Cell Proliferation & the Vascular System in a Transplanted Mouse Mammary Tumor. *Brit. J. Cancer* **22**, 258

Thomlinson, R.H. & Gray, L.H. (1955) The Histologic Structure of some Human Lung Cancers and the Possible Implications for Radiotherapy. *Brit. J. Cancer* **9**,

539

Vindelor, L.L., Christensen, I.J. & Nissen, N.I. (1983) A detergent-trypsin method for the preparation of Nuclei for flow cytometric DNA analysis. *Cytometry* **Vol. 3,** 323.

Yuhas, J.M.& Li, A.P. (1978) Growth fraction as the major determinant of multicellular tumor spheroid growth rates. *Cancer Res.* **38,** 1528.

LEGENDS

Fig. 1. Schematic of sandwich system. (a) Top view, showing two sandwiches in a Petri dish, with holders (cross-hatched) and spacers (solid black) at the left and right ends. Note the axes. The shaded region in the lower sandwich denotes the necrotic center; the dashed line divides the viable border into the two visibly different regions. (b) Edge view, showing the medium-filled gap between slides and cells attached to the bottom slide.

Fig. 2. Theoretical oxygen concentration as a function of distance x into the sandwich. f_a is the concentration at the edges of the slide (e.g. at $x=0$). Note that the oxygen profile is flat in the necrotic region, where there are no consuming cells.

Fig. 3. The growth curve of 9L cells. The points in the exponential region were fit by linear regression. This plot reflects three experiments. The standard deviation was within the plotted points.

Fig. 4. Glucose (▪) and lactic acid (×) concentrations for the exponential and confluent growth of 9L cells in monolayer. When no error bar is shown the standard deviation lies within the plotted points.

Fig. 5. Border widths X_b (○) and X_s (•) as functions of time. The first three points for X_s were fit by linear regression.

Fig. 6. Final border width as a function of gap size. Each point represents 15 replicate samples.

Fig. 7. Labelling index *versus* distance into the sandwich for 60μm (○), 180μm (+) and 290μm (▪) gap sandwiches, all at 48 hr. Arrows indicate the start of the necrotic region for the 60μm and 180μm cases. At 48 hr the 290μm sandwiches show no necrotic center. The standard deviations were within the plotted points.

Fig. 8. Representative DNA histograms for (a) exponentially growing cells and (b) 60μm gap sandwiches at 39 hr. Each histogram represents a total of 10^5 cells. The coefficients of

variation were less than 4%.

Table 1. Cell-cycle distributions; based on DNA content analysed by flow cytometry.

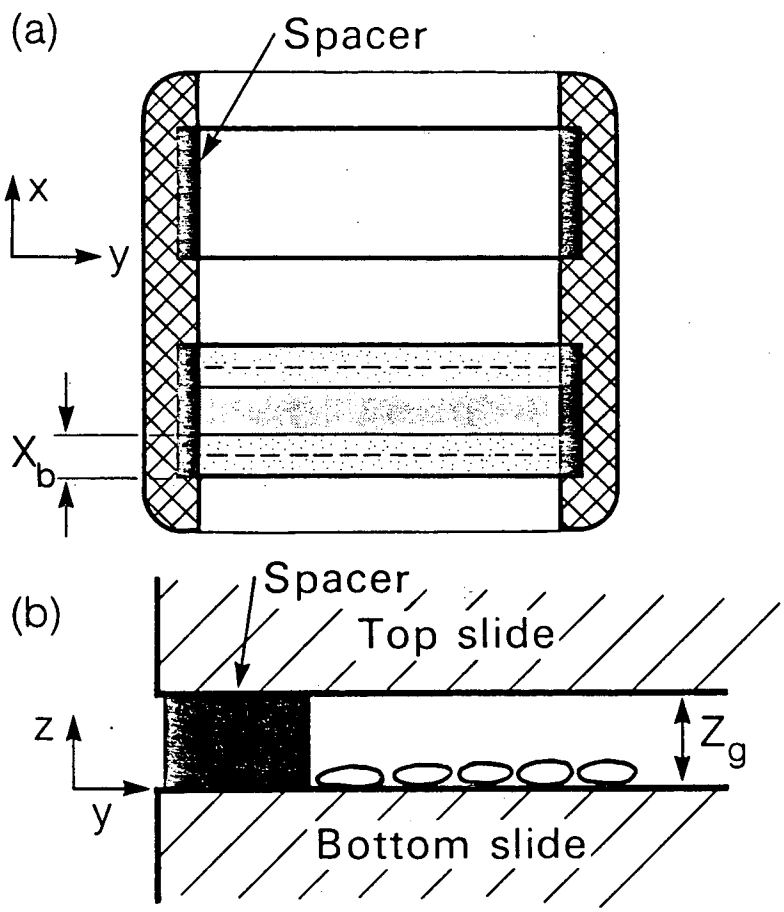

XBL 849-7979A

Fig. 1

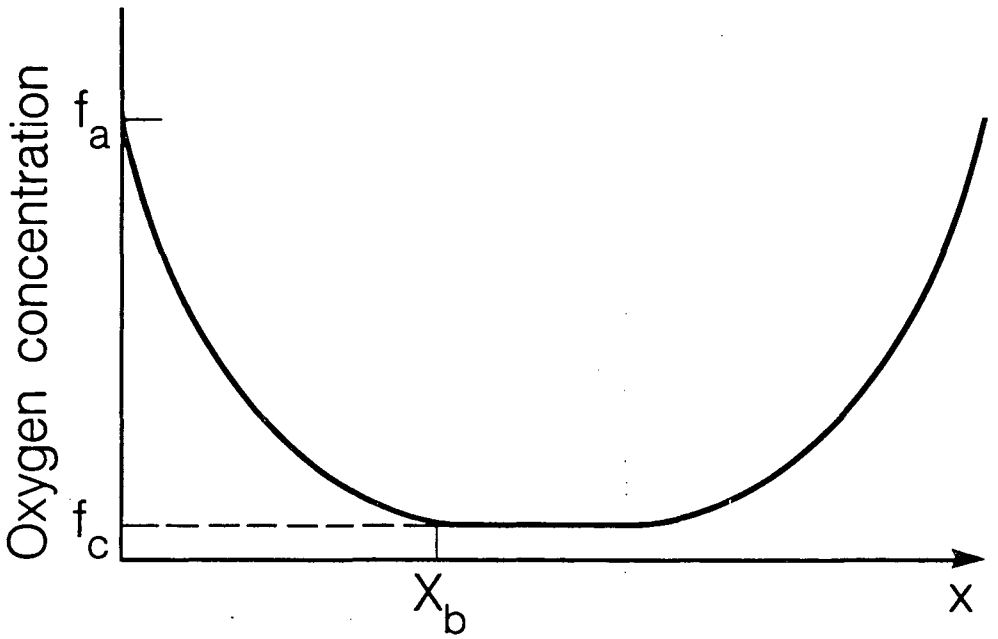

XBL 849-7978

Fig. 2

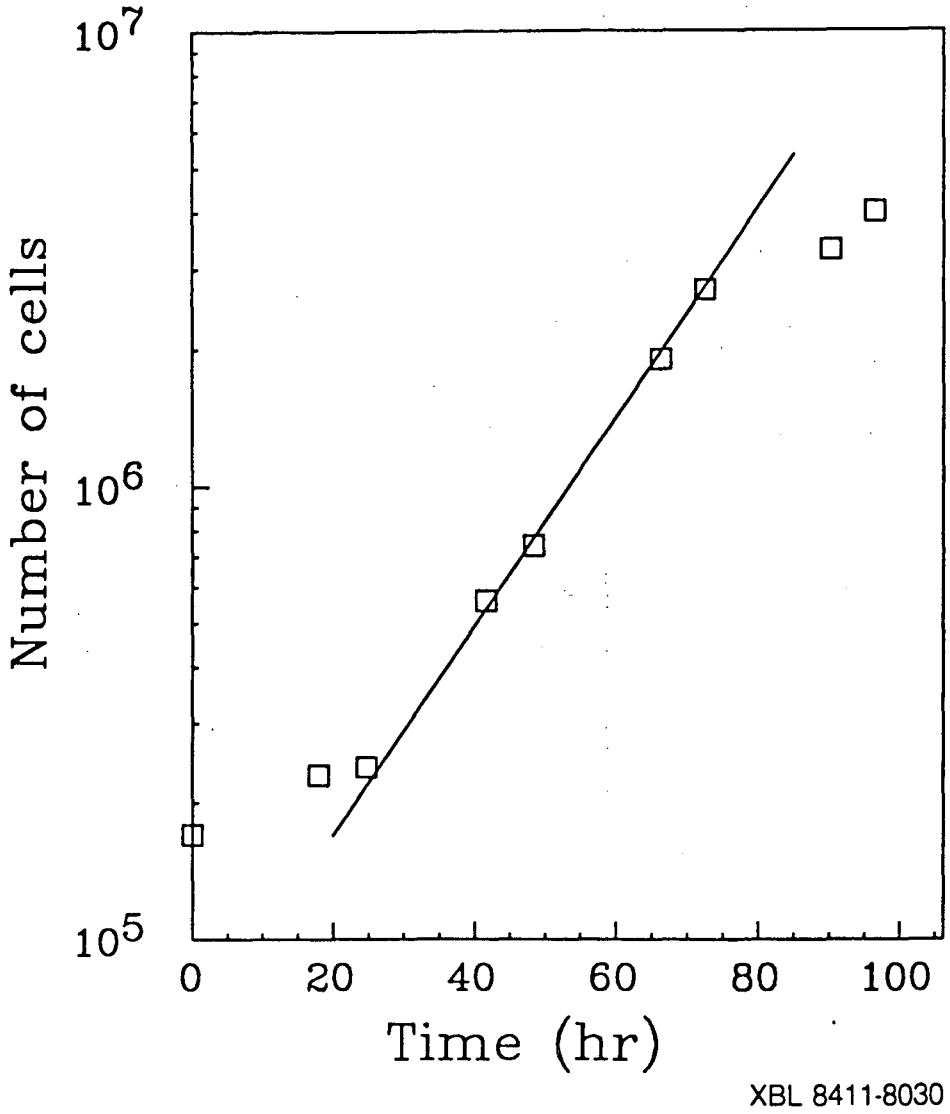
10^7
10^6
10^5
Number of cells
0
20
40
60
80
100
Time (hr)
XBL 8411-8030

Fig. 3

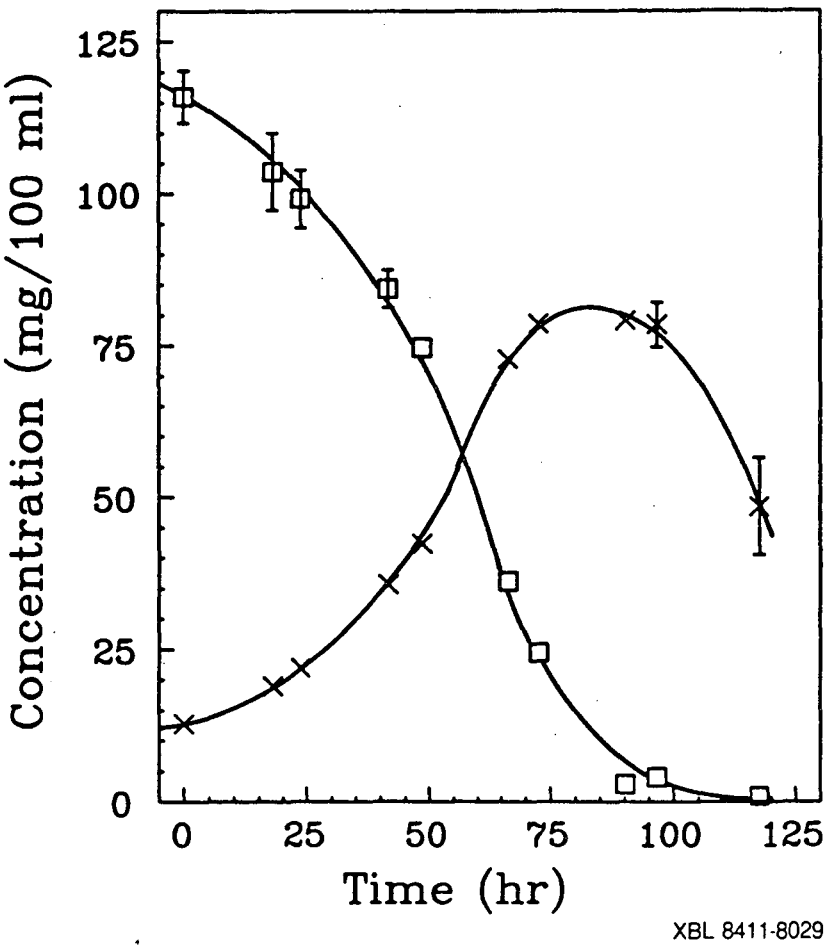
Concentration (mg/100 ml)
125
100
75
50
25
0
0
25
50
75
100
125
Time (hr)
XBL 8411-8029

Fig. 4

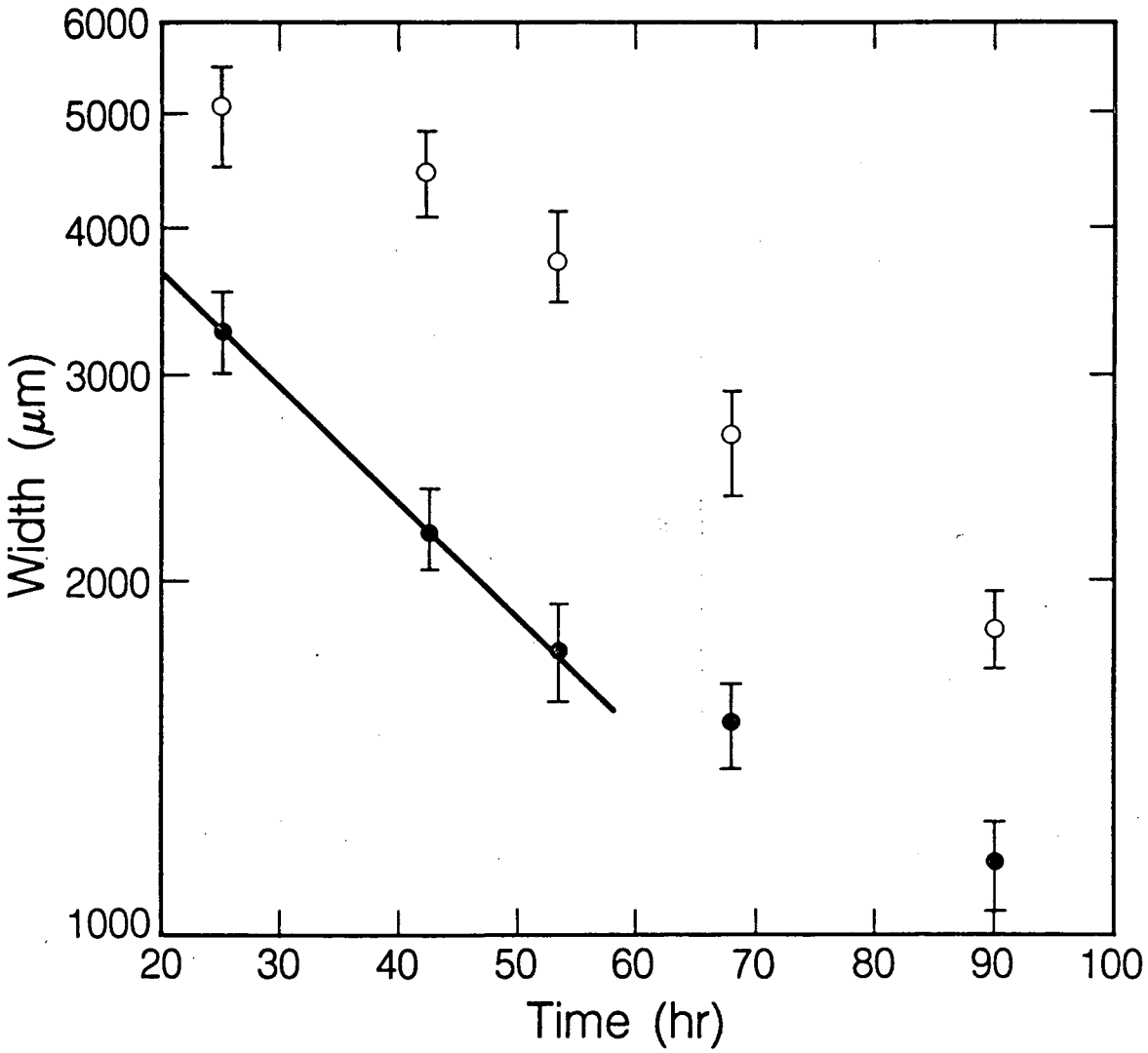

XBL 8411-8025

Fig. 5

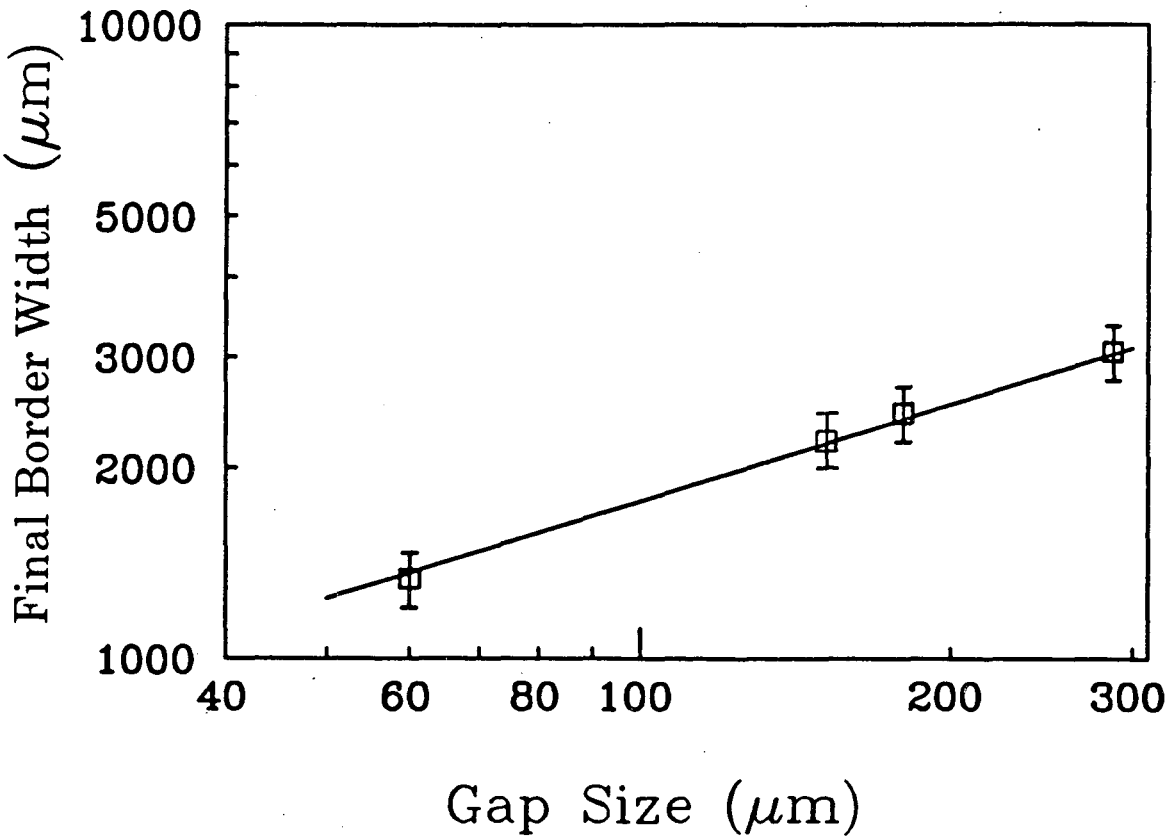

XBL 8411-8028

Fig. 6

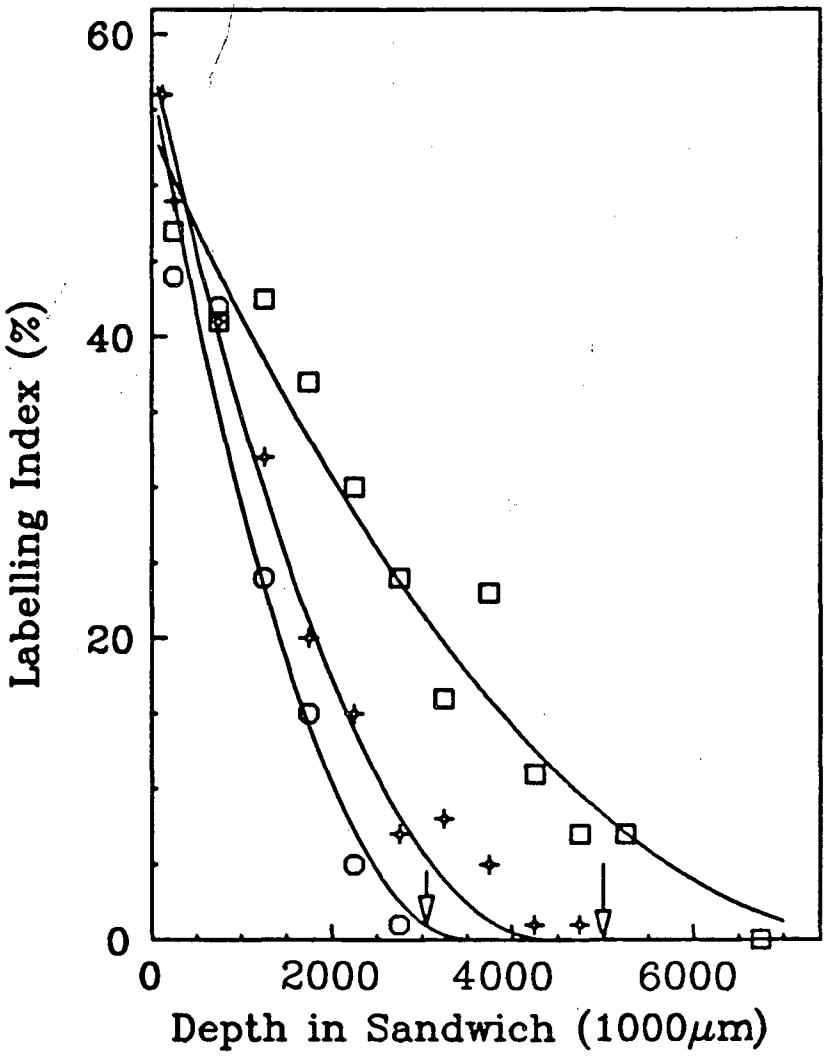
60
40
20
0
Labelling Index (%)
0
2000
4000
6000
Depth in Sandwich (1000μm)
XBL 8411-8026

Fig. 7

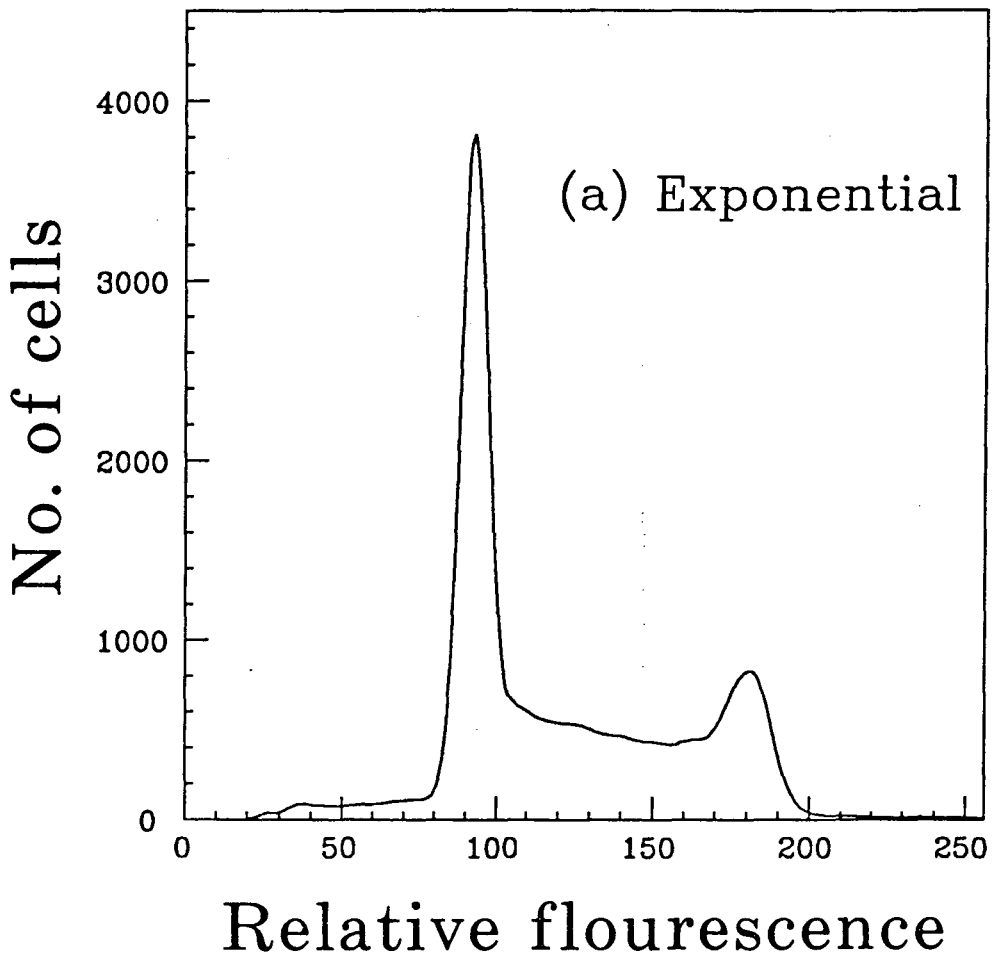

XBL 8411-8035A

Fig. 8 (a)

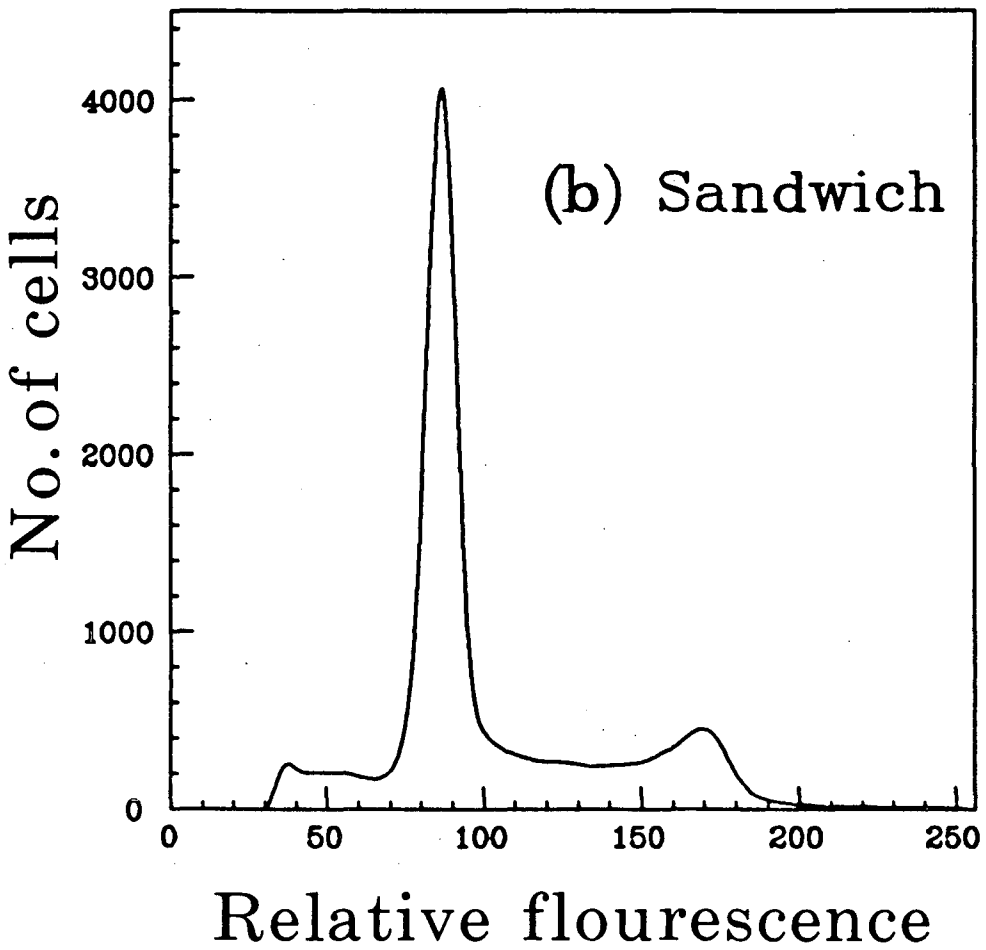
(b) Sandwich
No. of cells
4000
3000
2000
1000
0
0
50
100
150
200
250
Relative flourescence
XBL 8411-8027A

Fig. 8 (b)

System studied	G_0/G_1	S	G_2/M
Exponentially growing monolayer	42%	45%	13%
Sandwich: t = 22.5 hr	60	30	10
Sandwich: t = 39 hr	68	24	8
Confluent monolayer	86	9	5

Table 1

TECHNICAL INFORMATION DEPARTMENT
LAWRENCE BERKELEY LABORATORY
UNIVERSITY OF CALIFORNIA
BERKELEY, CALIFORNIA 94720